FABRICATION OF SPHERICAL NANOCRYSTALLINE $MnCo_2O_4$ VIA SOL- GEL CITRATE ROUTE FOR SUPERCAPACITOR APPLICATION

Santosh J Uke[1,2], Vijay P. Akhare[2], Satish P. Meshram[3], Devidas R. Bambole[1], Dindayal S. Thakre[1], Gajanan N. Chaudhari[2].

[1*]Department of Physics, J.D.P.S. College, Daryapur, Dist Amravati, Maharashtra, India,

[2]Nanoscience Research Laboratory, Shri. Shivaji Science College, Amravati, Maharashtra, India

[3]Nanomaterials Laboratory, Centre for Materials for Electronics Technology (C-MET), Pune, India

Abstract

Herein present paper, the sol-gel citrate route for synthesis of crystalline $MnCo_2O_4$ nanosphers is reported. The as- synthesized nanocrystalline $MnCo_2O_4$ were characterized by means of X-ray diffraction (XRD), Field emission scanning electron microscopy (FE-SEM), Fourier transform infrared spectroscopy (FTIR) and Brunauer–Emmett–Teller (BET). The XRD analysis reveals the nanocrystalline nature of as-prepared $MnCo_2O_4$ nanocrystals. Electrochemical properties of nanocrystalline $MnCo_2O_4$ have been studied by cyclic voltammetry, Galvanostatic charge–discharge and electrochemical impedance spectroscopy, which showed the maximum specific capacitance of 42.5 F g^{-1}at current density 0.1 $mAcm^{-2}$. The synthesis method used in this study is promising for producing the nanocrystalline material for high performance supercapacitor electrode.

Keywords: Nanocrystalline, capacitor, capacitance.

I. INTRODUCTION

To meet the recent and future challenges in the modern society, the flexible, wearable, lightweight and low cost energy storage system has a very intense demand [i]. In this regards, the world has an ample expectation from the scientific community for finding new energy storage system that fulfils these requirements. Recently, supercapacitor or electrochemical capacitor (EC) is the emerging energy storage systems are currently having intense demands. Supercapacitor is going to overcome the recent commercial energy storage like conventional capacitor and lead acid battery. Supercapacitor has many attractive features such as high power density, high energy density, lightweight, fast charging-discharging rate, a good shelf life, secure operation and long life span etc. [ii,iii]. The supercapacitor is used in various applications such as hybrid vehicles, military services and power backup, portable electronics like laptops, mobile phones, wrist watches, wearable devises, roll-up displays electronic papers, etc.[iv,v].

An electrode plays a very important role in the supercapacitor. Depending upon the electrode material used, the supercapacitors are divided into two categories: electrochemical double layer supercapacitor (EDLCs) and pseudocapacitor [vi]. In (EDLCs), the electrode material have been used as SWNT [vii], MWNT [viii], reduced graphine oxide [ix], porous carbon [x], etc., and the specific capacitance arises from the non-Faradaic charge storage mechanism between electrode and electrolyte interface. In pseudocapacitor, the electrode materials that have been used as electrode are transition metal oxides, and the specific capacitance arises from Faradaic reaction at the electrode interface [xi].

The transition metal oxides such as RuO_2, Fe_3O_4, Co_3O_4, MnO_2, Mn_3O_4, CeO_2, Fe_2O_3 etc., and the ternary metal such as $MnCo_2O_4$, $NiCo_2O_4$, $ZnFe_2O_4$, $ZnCo_2O_4$, $CoFe_2O_4$,

$CuFe_2O_4$ and $NiFe_2O_4$ etc., has been widely studied and employed as promising electrode material for pseudocapacitors [xii].

Among these ternary metal oxides, the $MnCo_2O_4$ is the most explored potential candidate in view point of electrode material for supercapacitor owing to its excellent electrochemical properties, natural abundance, cost effectiveness and environmentally compatible nature. In this context several researchers have reported the remarkable results. Sun *et. al.* [xiii] have reported the hydrothermally synthesized $MnCo_2O_4$/C electrode material for water splitting and all state solid supercapacitor application with high specific capacitance of 846 $mFcm^{-2}$ at current density 20μ A cm^{-2}.

Further, Yaun *et al.* [xiv] have reported the one step hydrothermal rout synthesis of $MnCo_2O_4$/reduced graphene oxide nanocomposites for supercapacitor with specific capacitance 334Fg^{-1} at current density 1Ag^{-1}. Sahoo *et al.* [xv] have reported the one-step electrodeposition approach for the synthesis of $MnCo_2O_4$ and reported the specific capacitance of 290 Fg^{-1} at scan rate 1mVs^{-1}.

In the present report, we have synthesized the $MnCo_2O_4$ via sol-gel citrate method. The synthesized material was characterized using XRD, FE-SEM, FTIR, UV-visible spectroscopy, BET-BJH etc. The electrochemical investigations for supercapacitor application of fabricated $MnCo_2O_4$ electrode was carried out using cyclic voltammetry, galvonostatic charge discharge and impedance spectroscopy.

II. EXPERIMENTAL

A. MATERIALS AND METHOD

All reagents including $KMnO_4$, $Co(NO_3)$ $6H_2O$ and citric acid ($C_6H_8O_7$) were used as starting material and purchased from Qualigen Sd. fine chemicals Ltd. India. The chemical reagents were of analytical grade and used as received.

B. Synthesis of crystalline $MnCo_2O_4$ nanosphere

Synthesis of nanocrystalline $MnCo_2O_4$was carried out by sol-gel citrate method. Initially, the stoichiometric amount of $KMnO_4$ and $Co(NO_3)$ $6H_2O$ with the molar ratio 1:2 were dissolved in methanol. This solution was stirred for 1 hr using a magnetic stirrer followed by vigorous stirring at 80°C on the hot plate for 3 hrs, which results in highly viscous homogenous thick gel. This gel was further transferred to a pressure bomb. The pressure bomb was sealed and heated up to 120°C for 12h and subsequently cooled to room temperature. The obtained dried samples were further ground and calcined at 550°C up to 6 h using alumina crucible in furnace.

C. FABRICATION OF ELECTRODE

The nanocrystalline $MnCo_2O_4$ material was loaded on stainless steel substrate following the standard protocol used for supercapacitor measurement [xvi,xvii]. For this, the 75 weight % of active material, 15 weight % acetylene black as a conductive additive and 10 weight % Poly vinylidene fluoride (PVDF) as a binder were mixed and ground in mortar to have a homogenous mixture. This mixture was further dispersed in a dimethyl formamide (DMF) to form slurry. This slurry was coated on stainless steel (SS) substrate using doctor blade and dried at 60°C. The electrochemical studies such as cyclic voltammetry, galvonostatic charge discharge and impedance spectroscopy were performed using the CHI 6002C and CHI 604E electrochemical workstation forming an electrochemical cell comprising fabricated electrode as working electrode, platinum as counter electrode and Ag/AgCl as a reference electrode in 1 M Na_2SO_4 electrolyte.

D. CHARACTERIZATION

The structural properties and phase identification of the samples was done by Philips X–ray diffractometer (XRD) with filtered Cu-K_α radiation of wavelength λ= 0.1541874 nm. The morphology was determined by Field emission scanning electron microscopy (FE–SEM) (Model: JSM 6701F, JEOL, Japan). The Fourier transform infrared (FTIR) spectra were recorded using Bruker vertex 70 FTIR spectrometer. The VU- Visible investigation of the material was carried out by using Perkin-Elmer Lamda 750, USA.

III. RESULT AND DISCUSSIONS

A. XRD analysis

To understand the lattice parameter and average crystallite size of the as–synthesized $MnCo_2O_4$ samples, the X-ray diffraction (XRD) analysis was carried out. Fig. 1 shows the typical XRD pattern of as-synthesized $MnCo_2O_4$. From the XRD pattern, the sharp peaks appearing at two theta values 31°, 36.95°, 44.44°, 52.07°, 58.18°, 64.52°, 66.9° and 76.85°

can be assigned to (222), (311), (400), (422), (511), (440), (531) and (533) respectively, and are in well agreement to those of spinel fcc structure with space group Fd3m, (227), [JCPDF 23-1237] [xviii,xix]. Further, no impurity peaks were found in the XRD pattern which indicates the formation of well crystalline $MnCo_2O_4$. The average crystallite size D was calculated using the Deby-Scherrer formula [xx] equation (1), where λ is the characteristic wavelength of Cu-Kα radiation, β is the full width half maxima of the diffraction line at half the maximum intensity and θ is the Braggs diffraction angle. The average crystalline size for the $MnCo_2O_4$ was found to be 32 nm.

$$D = \frac{0.9\lambda}{\beta \times \cos\theta} \quad (1)$$

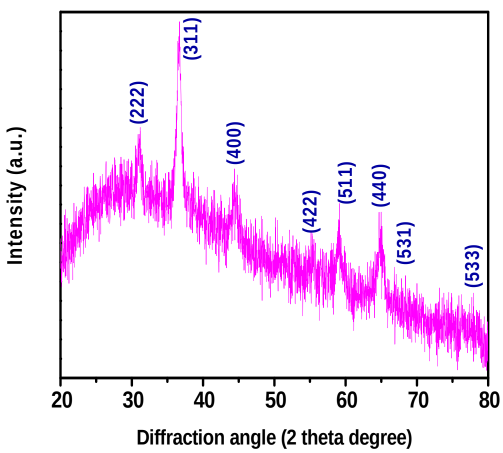

Fig. 1: XRD pattern of nanocrystalline $MnCo_2O_4$

B. FE-SEM analysis

The morphology of as-synthesized nanocrystalline $MnCo_2O_4$ was studied by FE-SEM analysis and the results are shown in Fig. 2. (a) and (b). From high magnification FESEM images (Fig 2(a)-(b)), it can be seen that the as-synthesized product consists of nearly spherical morphology. The nanospheres are formed in large numbers and are separated from each other. The average size of the nanospheres ranges from 29-42 nm which are in close agreement with those of XRD results.

The crystalline nature with spherical morphology of as-synthesized $MnCo_2O_4$ material demonstrated here may exhibit greater surface area and may contribute to electrolyte ion exchange which is one of the prime requirements of high energy storage supercapacitor electrode material.

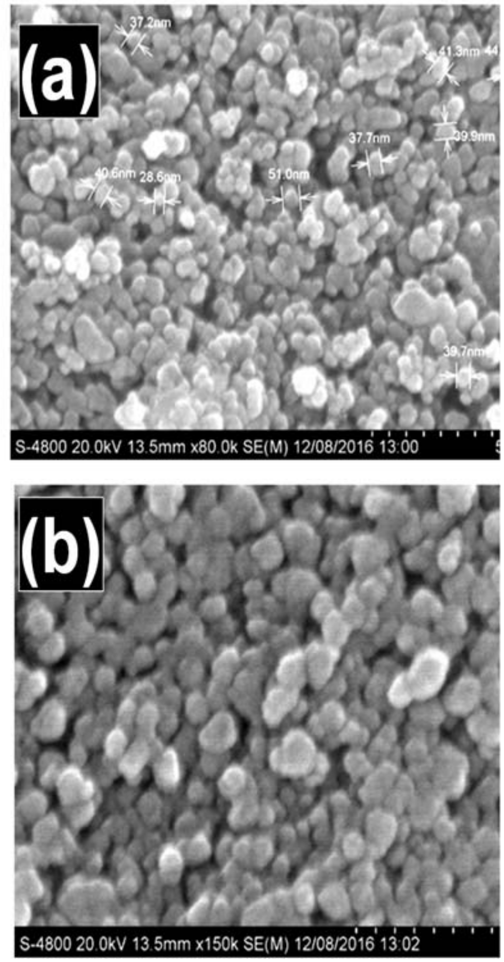

Fig. 2: FE-SEM micrograph of nanocrystalline $MnCo_2O_4$

C. FT-IR analysis

To analyze the bonding and chemical composition of the as synthesized nanocrystalline $MnCo_2O_4$, the Fourier transform infrared spectroscopy (FT-IR) analysis was carried. Fig. 3 shows the FT-IR spectrum of nanocrystalline $MnCo_2O_4$. The broad absorption peak appearing at 2922.59 cm^{-1} and 1609.7 cm^{-1} can be assigned to the O-H of adsorbed water molecule in $MnCo_2O_4$ [xxi,xxii]. The absorption band observed at 1348 cm^{-1} can be ascribed to NO_2 symmetrical stretching in the citrate molecule. The absorption bands at 750–600 cm^{-1} and 600–450 cm^{-1} are due to Mn–O stretching and bending vibrations in the nanocrystalline $MnCo_2O_4$ [xxiii]. The band at 720 cm^{-1} is due to NH_2 wagging from the citrate molecule [xxiv]. The band at680 cm^{-1} can be attributed to the metal oxide bonding [xxv].

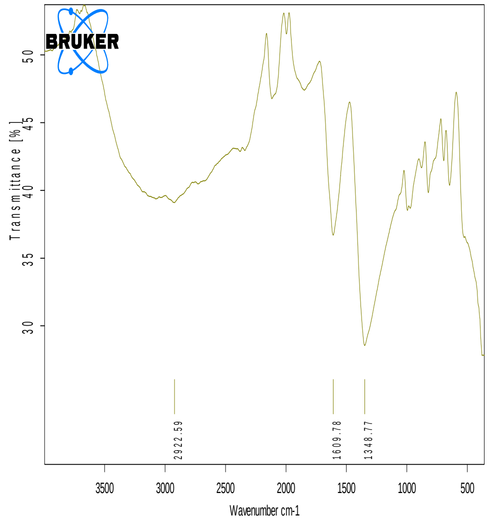

Fig. 3: FTIR spectrum of nanocrystalline $MnCo_2O_4$

D. UV- visible spectroscopy analysis

To investigate the optical band gap in the nanocrystalline $MnCo_2O_4$, the optical study of the as-synthesized nanocrystalline $MnCo_2O_4$ was carried out by using UV–vis spectrophotometer in the wavelength ranges 350–950 nm. The variation in absorption intensity with different wavelengths of nanocrystalline $MnCo_2O_4$ is shown in Fig. 4 (a) and corresponding plot of $(\alpha h\nu)^2$ versus (hν) shown in the Fig. 4 (b). The electronic structure and band gap strongly influences the electrochemical properties of the composite material. Fig. 4 (b) shows the strong absorption of nanocrystalline $MnCo_2O_4$ in the 220-250cm^{-1} region. The plot $(\alpha h\nu)^2$ versus (hν) (Fig. 4 (b)), which is linear at the absorption edge, further confirms that the material has a direct band gap. The extrapolations of straight line to the energy axis for zero absorption coefficient value give the band gap which was observed to be 4.91 eV. These values are comparable with the theoretical values previously reported in literature [xxvi].

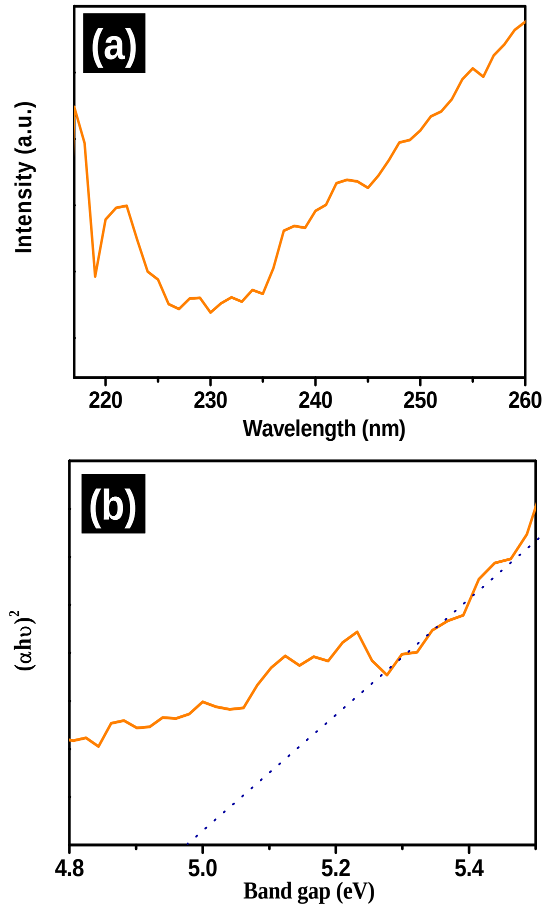

Fig. 4. (a) UV-Visible spectrum and (b) band gap of nanocrystalline $MnCo_2O_4$

E. BET surface area analysis

The Brunauer-Emmett-teller (BET) surface area analysis was carried out to explore the specific surface area of nanocrystalline $MnCo_2O_4$. For this, the N_2 adsorption-desorption isotherm has been carried out. The corresponding results are demonstrated in Fig. 5. From figure, the isotherm with a distinct hysteresis loop in the range of 0 to 1 and at relative pressure *P/Po* canbe clearly seen. The pore size distribution and pore volume of nanocrystalline $MnCo_2O_4$ are estimated using the Barrett-Joyner-Halenda (BJH) method. The pore size distribution of nanocrystalline $MnCo_2O_4$ at the amount of nitrogen absorbed at *P/Po* =0.98595 are shown in inset of Fig. 5. The BET surface area and a corresponding pore volume of the nanocrystalline $MnCo_2O_4$ were found out to be 10.45 m^2g^{-1} and 0.0213 cm^3g^{-1} respectively.

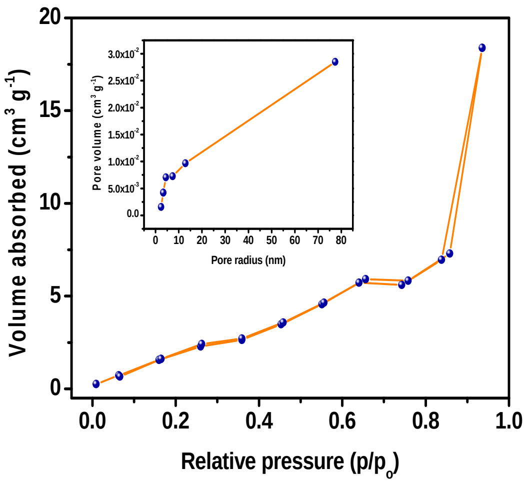

Fig. 5. N_2-adsorption desorption isotherm and the inset shows the corresponding pore size distribution of nanocrystalline $MnCo_2O_4$

F. Electrochemical characterizationanalysis

To understand the electrochemical nature of nanocrystalline $MnCo_2O_4$ electrode, the cyclic voltammetry (CV), galvonostatic charge discharge (GCD) and Electrochemical impedance spectroscopy (EIS) has been carried out in 1 M Na_2SO_4 as electrolyte. The Fig. 6 (a) shows the CV curves of nanocrystalline $MnCo_2O_4$ in the different scan rates of 5 mVs^{-1}, 10 mVs^{-1}, 50 mVs^{-1} and 100 mVs^{-1} in the potential window 0 to 0.6V. The rectangular shape of CV reveals that the specific capacitance is originated from the redox reaction [xxvii]. From CV curves, the values of specific capacitance of nanocrystalline $MnCo_2O_4$ samples at different scan rate are calculated using the equation (2).

$$C_s = \frac{1}{mV(V_c - V_a)} \int_{V_a}^{V_c} I(V)dV \qquad (2)$$

Where *m* is the mass in (gcm^2) deposited, *I(v)* is the response current in (mA) of the $MgFe_2O_4$electrode for unit area, *V* is the scan rate, $(V_c - V_a)$ is the operational potential window in (V), V_a anodic current and V_c cathodic current.

Galvonostatic charge-discharge study of the electrodes of $MnCo_2O_4$ electrode at different current densities 0.1 to 0.5 $mAcm^{-2}$ has been studied using 1M Na_2SO_4 as electrolyte. Fig.6 (b) shows the galvonostatic charge discharge behaviour of the nanocrystalline $MnCo_2O_4$ electrode. The discharge specific capacitance was calculated by galvonostatic charge discharge curves using the equation (3). Additionally, the galvonostatic charge discharge curve is used to measure the energy density and power density of the electrode material, an equation (4) and equation (5) were used to calculate the energy density E ($W\ h\ Kg^{-1}$) and power density P ($W\ Kg^{-1}$) respectively,

$$C_s = \frac{T_d \times I_d}{m \times \Delta V} \qquad (3)$$

$$E = \frac{0.5 \times C_s \times (V_{\max}^2 - V_{\min}^2)}{3.6} \qquad (4)$$

$$P = \frac{E \times 3600}{T_d} \qquad (5)$$

Where Cs (Fg^{-1}) is the specific capacitance, I_d (A) is the current used for Galvonostatic discharge, T_d (s) discharging time, ΔV(V) potential window used for galvonostatic charge discharge and m(g) is the active mass of the electrode [xxviii]. From GCD, the maximum specific capacitance, energy density and power density of $MnCo_2O_4$ electrode at current density 0.1$mAcm^{-2}$ has obtained as 42.5 Fg^{-1}, 2.125W h Kg^{-1} and 137.1kW Kg^{-1}, respectively. Adekunle *et. al.* [xxix] have reported the specific capacitance 11.76 Fg^{-1} for the MWCNT-Co_3O_4/MWCNT asymmetric supercapacitor assembly in 1 M Na_2SO_4. In present reports, the specific capacitance for $MnCo_2O_4$ electrode at current density 0.1mA cm^{-1} was found out to be 42. 5 Fg^{-1}, which is high in comparison with the specific capacitance reported in the literature.

Further, the retention of specific capacitance of the $MnCo_2O_4$ electrode was examined at the current density 0.3 $mAcm^{-2}$ over 1000 cycles. Fig 7 (a) shows the curve for cycle number versus percentage capacity retention for $MnCo_2O_4$ electrode. From figure, it can be seen that the $MnCo_2O_4$ electrode shows the 95.23% retention of specific capacitance over 1000 cycles.

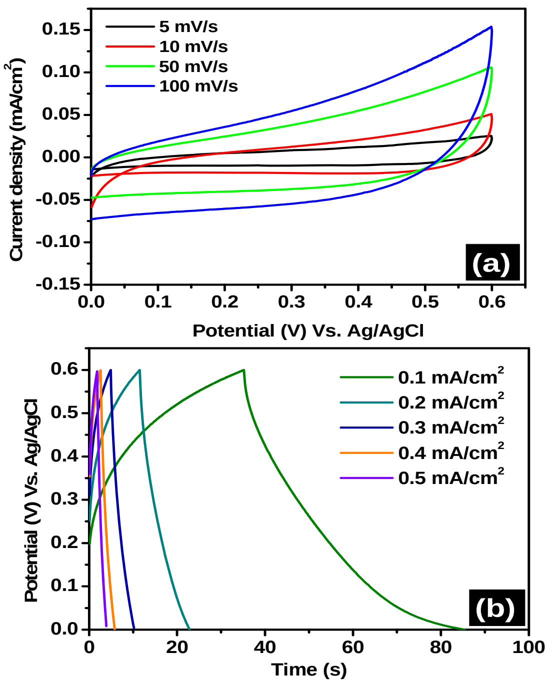

Fig. 6. (a) Cyclic voltammogram (CV), (b) Galvonostatic charge discharge (GCD) of nanocrystalline $MnCo_2O_4$

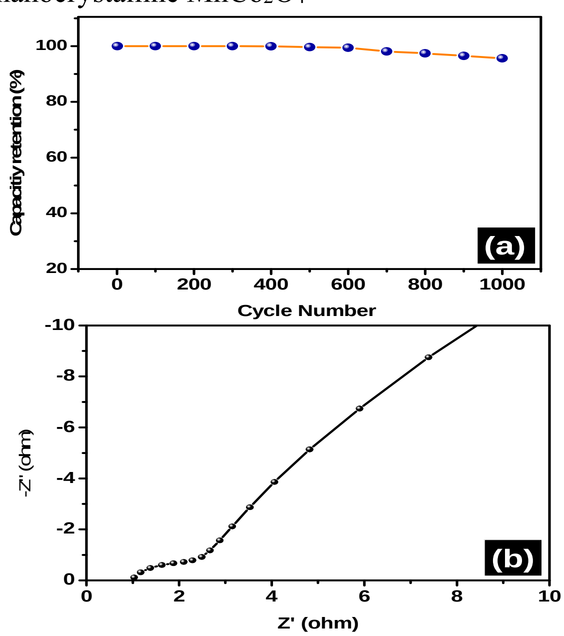

Fig. 7. (a) Capacity retention vs. cycle number at 0.3 $mAcm^{-2}$ and (b) Nyquist plot of nanocrystalline $MnCo_2O_4$

The electrolyte resistance (R_s), the charge–transfer resistance (R_{ct}), the ion transport properties within the interface between the electrode and electrolyte was investigated with the help of electrochemical impedance spectroscopy (EIS). The ESI was investigated within the frequency range 1 Hz to 1 MHz at AC amplitude of 5 mV in 1 M Na_2SO_4 electrolyte.

The typical Nyquist plot for the $MnCo_2O_4$ nanostructure is shown in Fig. 7 (b). The high–frequency intercept of the semi–circle on the real axis yields the electrolyte resistance (R_s) or equivalent series resistance, and the diameter provides the charge–transfer resistance (R_{ct}) over the interface between the electrode and electrolyte [xxx]. The electrolyte resistance (R_s), the charge–transfer resistance (R_{ct}), of the nanostructure $MnCo_2O_4$ was found out to be 2 Ωcm^{-2} and 1.24 Ωcm^{-2}respectively. The low electrolyte resistance(R_s) and the charge–transfer resistance (R_{ct}) of the electrode material are mostly responsible for the result of ion exchange between electrode and electrolyte interface [xxxi]. Fig.8 (a) shows the Bode plot (Phase (Ω cm^{-2}) vs. Frequency (Hz)) of as-synthesized $MnCo_2O_4$ nanostructure.

At low frequency, the phase angle of the electrodes reached to the 45^o implies the idea capacitive behavior of the electrode. The characteristic frequency f_o of a phase angle of 45^o is ~100 Hz for the $MnCo_2O_4$ nanostructure. The relaxation time constant t_o, is calculated from the equation t_o=1/f_o, it was found out to be ~ 0.01. Thus, ESI analysis of nanostructure $MnCo_2O_4$ is in good agreement with the results obtained from CV and GCD.

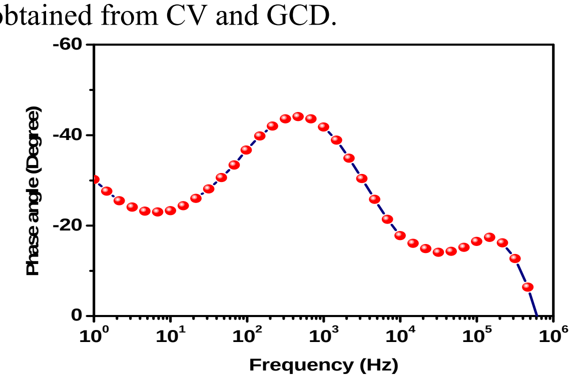

Fig.8 (a) shows the Bode plot (Phase (Ω cm^{-2}) vs. Frequency (Hz)) for nanostructure $MnCo_2O_4$

IV. CONCLUSION

In conclusion, we have successfully synthesized the nanocrystalline $MnCo_2O_4$ via cost effective sol-gel citrate method. The nanocrystalline $MnCo_2O_4$ shows the excellent electrochemical performance in 1M Na_2SO_4 electrolyte. The electrochemical impedance spectroscopy reveals that the nanocrystalline $MnCo_2O_4$ is promising electrode material for high performance supercapacitor. Moreover, the present study demonstrates simple, cost effective sol-gel citrate method for fabrication of uniform nanocrystalline $MnCo_2O_4$ with very high potential as the electrode for supercapacitor.

V. ACKNOWLEDGMENT

This work is financially supported by University Grant Com-mission (UGC) New Delhi, India under Minor Research Project (File No.47-763/13/WRO) and (File No.47-764/13/WRO).

VI. REFERENSE

[1] Saha, S., Jana, M., Khanra, P., Samanta, P., Koo, H., Murmu, N. C., & Kuila, T. (2016). Band gap modified boron doped NiO/Fe 3 O 4 nanostructure as the positive electrode for high energy asymmetric supercapacitors. RSC Advances, 6(2), 1380-1387.

[2] Uke, S. J., Akhare, V. P., Bambole, D. R., Bodade, A. B., & Chaudhari, G. N. (2017). Recent Advancements in the Cobalt Oxides, Manganese Oxides, and Their Composite As an electrode Material for Supercapacitor: A Review. Frontiers, 4(21), 1

[3] Jayalakshmi, M., & Balasubramanian, K. (2008). Simple capacitors to supercapacitors-an overview. Int. J. Electrochem. Sci, 3(11), 1196-1217..

[4] Wang, G., Lu, X., Ling, Y., Zhai, T., Wang, H., Tong, Y., & Li, Y. (2012). LiCl/PVA gel electrolyte stabilizes vanadium oxide nanowire electrodes for pseudocapacitors. ACS nano, 6(11), 10296-10302.

[5] Lee, S. W., Gallant, B. M., Byon, H. R., Hammond, P. T., & Shao-Horn, Y. (2011). Nanostructured carbon-based electrodes: bridging the gap between thin-film lithium-ion batteries and electrochemical capacitors. Energy & Environmental Science, 4(6), 1972-1985

[6] Uke, S. J., Akhare, V. P., Bambole, D. R., Bodade, A. B., & Chaudhari, G. N. (2017). Recent Advancements in the Cobalt Oxides, Manganese Oxides, and Their Composite As an electrode Material for Supercapacitor: A Review. Frontiers, 4(21), 1.

[7] Liu, T., & Kumar, S. (2006). U.S. Patent No. 7,061,749. Washington, DC: U.S. Patent and Trademark Office.

[8] Huang, K. J., Wang, L., Zhang, J. Z., Wang, L. L., & Mo, Y. P. (2014). One-step preparation of layered molybdenum disulfide/multi-walled carbon nanotube composites for enhanced performance supercapacitor. Energy, 67, 234-240.

[9] Zhang, J., & Zhao, X. S. (2012). Conducting polymers directly coated on reduced graphene oxide sheets as high-performance supercapacitor electrodes. The Journal of Physical Chemistry C, 116(9), 5420-5426.

[10] Kang, D., Liu, Q., Gu, J., Su, Y., Zhang, W., & Zhang, D. (2015). "Egg-Box"-assisted fabrication of porous carbon with small mesopores for high-rate electric double layer capacitors. ACS nano, 9(11), 11225-11233.

[11] Shen, L., Yu, L., Yu, X. Y., Zhang, X., & Lou, X. W. D. (2015). Self-templated formation of uniform NiCo2O4 hollow spheres with complex interior structures for lithium-ion batteries and supercapacitors. Angewandte Chemie International Edition, 54(6), 1868-1872.

[12] Vadiyar, M. M., Bhise, S. C., Kolekar, S. S., Chang, J. Y., Ghule, K. S., & Ghule, A. V. (2016). Low cost flexible 3-D aligned and cross-linked efficient ZnFe 2 O 4 nano-flakes electrode on stainless steel mesh for asymmetric supercapacitors. Journal of Materials Chemistry A, 4(9), 3504-3512.

[13] Sun, C., Yang, J., Dai, Z., Wang, X., Zhang, Y., Li, L., ... & Dong, X. (2016). Nanowires assembled from MnCo2O4@ C nanoparticles for water splitting and all-solid-state supercapacitor. Nano Res, 9, 1300-1309.

[14] Yuan, Y., Bi, H., He, G., Zhu, J., & Chen, H. (2013). A facile hydrothermal synthesis of a MnCo2O4@ reduced graphene oxide nanocomposite for application in supercapacitors. Chemistry Letters, 43(1), 83-85.

[15] Sahoo, S., Naik, K. K., & Rout, C. S. (2015). Electrodeposition of spinel MnCo2O4 nanosheets for supercapacitor applications. Nanotechnology, 26(45), 455401.

[16] Biswal, M., Banerjee, A., Deo, M. and Ogale, S., 2013. From dead leaves to high energy density supercapacitors. Energy & Environmental Science, 6(4), pp.1249-1259.

[17] Yang, X., Sun, H., Zhang, L., Zhao, L., Lian, J. and Jiang, Q., 2016. High Efficient Photo-Fenton Catalyst of α-Fe2O3/MoS2 Hierarchical Nanoheterostructures: Reutilization for Supercapacitors. Scientific reports, 6, p.31591.

[18] Krishnan, S. G., Reddy, M. V., Harilal, M., Vidyadharan, B., Misnon, I. I., Ab Rahim, M. H., ... & Jose, R. (2015). Characterization of

MgCo 2 O 4 as an electrode for high performance supercapacitors. Electrochimica Acta, 161, 312-321.

[19] Liu, H., & Wang, J. (2012). Hydrothermal synthesis and electrochemical performance of MnCo2O4 nanoparticles as anode material in lithium-ion batteries. Journal of electronic materials, 41(11), 3107-3110.

[20] Warren, B.E. and Averbach, B.L., 1952. The separation of cold-work distortion and particle size broadening in X-ray patterns. Journal of Applied Physics, 23(4), pp.497-497.

[21] Raut, S. S., & Sankapal, B. R. (2016). First report on synthesis of ZnFe 2 O 4 thin film using successive ionic layer adsorption and reaction: approach towards solid-state symmetric supercapacitor device. Electrochimica Acta, 198, 203-211.

[22] Infrared spectroscopy : Fundamental and application ;Barbara Stuart, Wiley

[23] Sun, M., Ye, F., Lan, B., Yu, L., Cheng, X., Liu, S., & Zhang, X. (2012). One-step Hydrothermal Synthesis of Sn-doped OMS-2 and Their Electrochemical Performance. Int. J. Electrochem. Sci, 7, 9278-9289.

[24] Shinde, S. S., Gund, G. S., Dubal, D. P., Jambure, S. B., & Lokhande, C. D. (2014). Morphological modulation of polypyrrole thin films through oxidizing agents and their concurrent effect on supercapacitor performance. Electrochimica Acta, 119, 1-10.

[25] Ma, L., Shen, X., Ji, Z., Cai, X., Zhu, G., & Chen, K. (2015). Porous NiCo 2 O 4 nanosheets/reduced graphene oxide composite: Facile synthesis and excellent capacitive performance for supercapacitors. Journal of colloid and interface science, 440, 211-218..

[26] Habibi, M. H., & Fakhri, F. (2017). Hydrothermal synthesis of nickel iron oxide nano-composite and application as magnetically separable photocatalyst for degradation of Solar Blue G dye. Journal of Materials Science: Materials in Electronics, 1-6.

[27] Dubal, D. P., Chodankar, N. R., Holze, R., Kim, D. H., & Gomez-Romero, P. (2017). Ultrathin Mesoporous RuCo2O4 Nanoflakes: An Advanced Electrode for High-Performance Asymmetric Supercapacitors. ChemSusChem, 10(8), 1771-1782.

[28] Xu, K., Yang, J., Li, S., Liu, Q. and Hu, J., 2017. Facile synthesis of hierarchical mesoporous NiCo 2 O 4 nanoflowers with large specific surface area for high-performance supercapacitors. Materials Letters, 187, pp.129-132.

[29] Agboola, B. O., Ebenso, E. E., Oyenkunle, J. A., & Oluwatobi, O. S. (2015). Comparative supercapacitive properties of asymmetry two electrode coin type supercapacitor cells made from MWCNTS/cobalt oxide and MWCNTs/iron oxide nanocomposite.

[30] Dubal, D. P., Lee, S. H., Kim, J. G., Kim, W. B., & Lokhande, C. D. (2012). Porous polypyrrole clusters prepared by electropolymerization for a high performance supercapacitor. Journal of Materials Chemistry, 22(7), 3044-3052.

[31] Xu, K., Yang, J., Li, S., Liu, Q., & Hu, J. (2017). Facile synthesis of hierarchical mesoporous NiCo 2 O 4 nanoflowers with large specific surface area for high-performance supercapacitors. Materials Letters, 187, 129-132